Molecular dynamics of a classical lattice gas: Transport properties and time correlation functions

J. Hardy and O. de Pazzis
Laboratoire de Physique des Plasmas, Associé au C.N.R.S., Bâtiment 212, Université Paris XI, 91405 Orsay Cedex, France

Y. Pomeau
Service de Physique Théorique, Orme des Merisiers, C.E.A. 91400, Saclay, France

(Received 29 December 1975)

A study of the dynamics of a discrete two-dimensional system of classical particles is presented. In this model, dynamics and computations may be done exactly, by definition. The equilibrium state is investigated and the Navier-Stokes hydrodynamical equations are derived. Two hydrodynamical modes exist in the model: the sound waves and a kind of vorticity diffusion. In the Navier-Stokes equations one obtains a transport coefficient which is given by a Green-Kubo formula. The related time correlation function has been calculated in a numerical simulation up to a time of the order of 50 mean free flights. After a short time of exponential decay this time correlation behaves like t^{-S}, the exponent being compared to theoretical predictions.

I. INTRODUCTION

This paper is devoted to the dynamical properties of a simple model of classical particles moving on a two-dimensional lattice. Some exact properties of this model have been already investigated[1]; however, we have not yet been able to obtain any exact result concerning the long-time behavior of the time correlation functions. At the present time, the investigations on the convergence of the Green-Kubo formulas are realized only by approximate methods such as the mode-mode coupling theory[2] or the data derived from numerical simulations.

The problem of the long-time behavior of correlation functions involves the dynamical properties of many-body systems at a very detailed level.[3] It is then meaningful to focus attention on very simple models for which one can expect to find exact results. The present work takes place in this direction; in particular, computational results are compared with two kinds of theoretical predictions obtained from exact and approximate methods.[1]

Section II is devoted to the description of the model. In Sec. III the equilibrium properties and the hydrodynamical laws (Euler and Navier-Stokes) are reviewed. The Navier-Stokes hydrodynamical equations are derived from a phenomenological point of view, and the Green-Kubo formula giving the transport coefficient of the model is obtained through the Landau-Lifshitz fluctuating hydrodynamics. We give in Sec. IV the details of the numerical processes; owing to the special nature of the model presented here, many simplifications have been used for both dynamics and boundary conditions.

The results show explicitly that the long-time behavior of the correlation functions is proportional to t^{-S}; the experimental values of S are compared with the predicted ones.

II. DESCRIPTION

The model described in this section has been partly studied in a previous paper.[1] For practical reasons, we shall modify a little bit the definitions given there.

At time $t = 0$, all particles lie on the vertices of a square lattice. They are indistinguishable, which means that particles do not carry a label through time. In other words, we can say that at a given time a particle lies at some place with a given velocity, but we are unable (at least without some modification of the model) to say surely where this particle was at a given previous time, even if the complete dynamics are exactly known. This point will appear more clearly after the detailed description that follows. The mass of each particle is the unit mass, and their kinetic energy is $\frac{1}{2}$. The velocity of any particle points toward one of the four directions of the square lattice. We chose to avoid "molecles" on a vertex (i.e., situations where two particles with identical velocities coexist at the same place); in fact, collision laws should be given, in this case, between all kinds of molecules, which complicates the dynamics.

If at time $t = 0$ there is no molecule, the laws of the motion can be chosen so that such molecules never appear at any time. Thus at most four particles can lie on the same vertex, provided they have different velocities. We then have sixteen possible situations at a vertex, as given in Fig. 1.

An allowed set of positions and velocities of the particles on the lattice will be called a configuration, defined by a matrix E with integer elements E_{ij}. We have in binary scale

$$0 \leq E_{ij} \leq 1111. \tag{2.1}$$

The indices i, j denote a site on the lattice at the intersection of the ith column and the jth row.

Let us remark that in Fig. 1 the sixteen situations at a vertex are labeled by an ordered set of four digits equal to zero or one,

$$E_{ij} = d_{ij}\, c_{ij}\, b_{ij}\, a_{ij}. \tag{2.2}$$

The binary notation is the most natural way to define situation at a vertex, since 1 represents a particle and 0 a hole, the rank of this digit in the four-digit number E_{ij} being devoted arbitrarily to one of the four velocity directions (see Fig. 2).

Let us now define the procedure which, if a configuration is given at time t, enables one to build up the configuration at time $t+1$. We shall divide this procedure into two steps, a collision (velocities may change but particles stay at the same place) and a free translation (particles move from one site to a neighboring one, but their velociy remains unchanged). The first operation is performed by exchanging on every vertex of the lattice the situations 0101 and 1010 (see Fig. 1), the other situations remaining the same. Denoting as above by i and j the column and row indices, the effect of collision on the matrix E may be described by the operator C such as:

$$(\hat{C}E)_{ij} = \begin{cases} 0101, & \text{if } E_{ij} = 1010, \\ 1010, & \text{if } E_{ij} = 0101, \\ E_{ij}, & \text{otherwise.} \end{cases} \tag{2.3}$$

The second step of the time evolution may be called free motion; each particle makes one step forward in the direction of its velocity. The free translation operator T_0 describing this procedure acts on E as follows:

$$(T_0 E)_{ij} = d_{i\,j+1}\, c_{i+1\,j}\, b_{i\,j-1}\, a_{i-1\,j}, \tag{2.4}$$

with

$$E_{ij} = d_{ij}\, c_{ij}\, b_{ij}\, a_{ij}.$$

Denoting by T the evolution operator of one time step, by definition

$$T = T_0 \hat{C}. \tag{2.5}$$

The conservation of the number of particles and of the momentum are fulfilled by this evolution law; the conservation of the kinetic energy follows obviously from the conservation of the number of particles. Furthermore, situations where on a vertex two particles have the same velocities (i.e., "molecules," according to our previous definition) can never appear, since neither $\hat{C}$ nor T create separately such molecules.

The simplicity of the model makes some properties appear which makes it quite different from fluids with continuous velocities and positions. Some of these qualitative differences are obvious, but we shall consider in more detail two of them which are of some importance. First the dynamics do not have the property of microreversibility. In fact, denoting by Q the operation of reversing all velocities,

$$(QE)_{ij} = b_{ij}\, a_{ij}\, d_{ij}\, c_{ij}, \quad \text{for every } i, j; \tag{2.6}$$

thus, for example, $Q((1001)_{ij}) = (0110)_{ij}$. The microreversibility should imply, in terms of Q,

$$QT = T^{-1}Q. \tag{2.7}$$

It can be seen that this is not the case for our model; a counterexample is given in Fig. 3.

However, by extending the definition of the model to incorporate intermediate real times (instead of integer ones), one recovers the property of microreversibility. Let us suppose that between two neighboring integer values of time, particles have a rectilinear motion with a constant velocity. Denoting by $\vec{r}\,(t_0)$ the position of a particle at an integer time t_0, one can define the position of the same particle at any real time $t_0 \leq t \leq t_0 + 1$ by

$$\vec{r}(t) = \vec{r}(t_0) + (t - t_0)[\vec{r}(t_0 + 1) - \vec{r}(t_0)]. \tag{2.8}$$

The free motion operator T_0 describes the translation between two neighboring integer values of time; let us denote the translation defined by

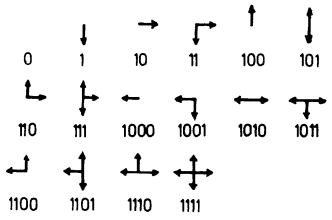

FIG. 1. Possible situations at a vertex.

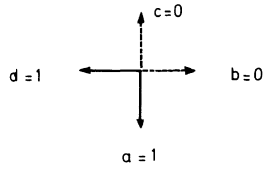

FIG. 2. Situation 1001; two particles, two holes.

(2.8) by the operator $T_0^{t-t_0}$. The evolution operator between $t_0+\xi$ and $t_0+\xi+1$ (ξ real, $0<\xi<1$) reads

$$K = T_0^{\xi-1}\, T\, T_0^{\xi} \tag{2.9}$$

and verifies the relation

$$QK = K^{-1}Q, \tag{2.10}$$

which means that the model is microreversible for any real noninteger times.

Let us consider now another pecularity of this model. The impact parameter is always zero in collisions; thus the total velocity is not only conserved on the whole lattice but its horizontal component is conserved on each row and its vertical component on each column.

The asymptotic time behavior of the Green-Kubo integrand (to be defined in Sec. III) is related in a crucial way[1] to the dimensionality of the system, and owing to the pecularity explained above, the Green-Kubo integrand behaves asymptotically as in a one-dimensional model.

III. THERMODYNAMICS AND HYDRODYNAMICS

In this section the model is supplied with an equilibrium measure and the Navier-Stokes hydrodynamical equations are derived. We tried to give a simple approach to the transport phenomena in the model, the derivation of rigourous results being not within the scope of this paper. Let us begin our study by the definition of a positive measure P which assigns to any configuration E a probability of existence $P(E)$, where

$$\sum_{E\in\{E\}} P(E) = 1, \tag{3.1}$$

with $P(E)\geq 0$, for every E, where $\{E\}$ is the finite set of the allowed configurations on a finite lattice. Writing as above the values of E_{ij} in binary notation, we may define for a given measure $P(E)$ four quantities which are, roughly speaking, the probability of finding a particle at point (i,j) with a velocity in the α direction ($\alpha\in\{1,2,3,4\}$),

$$N_1(i,j) = \sum_{E\in\{E\}} P(E)\, a_{ij}(E), \tag{3.2a}$$

$$N_2(i,j) = \sum_{E\in\{E\}} P(E) b_{ij}(E), \tag{3.2b}$$

$$N_3(i,j) = \sum_{E\in\{E\}} P(E) c_{ij}(E), \tag{3.2c}$$

$$N_4(i,j) = \sum_{E\in\{E\}} P(E) d_{ij}(E). \tag{3.2d}$$

As the quantities $a_{ij}, b_{ij}, c_{ij}, d_{ij}$ are equal to 0 or 1, then $0\leq N_\alpha\leq 1$ for $1\leq\alpha\leq 4$.

From the N_α we may define the mean density $n(i,j)$ and the mean current density at a given vertex,

$$n(i,j) = \sum_{\alpha=1}^{4} N_\alpha(i,j), \tag{3.3a}$$

$$J_x(i,j) = N_1(i,j) - N_3(i,j), \tag{3.3b}$$

$$J_y(i,j) = N_2(i,j) - N_4(i,j). \tag{3.3c}$$

J_x and J_y may be considered as the Cartesian components of a vector $\vec{J}$ in the plane of the lattice.

The inequalities

$$0\leq N_\alpha\leq 1, \quad \text{for each } \alpha\in\{1,2,3,4\}, \tag{3.4}$$

lead to some restrictions in the range of variation of the density and of the current density,

$$0\leq n\leq 4, \tag{3.5a}$$

$$|J_x|\leq 1, \quad |J_y|\leq 1, \tag{3.5b}$$

$$|J_x| + |J_y| \leq \min(n, 4-n). \tag{3.5c}$$

It can be shown[1] that for every $(n,\vec{J})$ satisfying the inequalities (3.5) an equilibrium or invariant measure P_0 exists.

Because the impact parameter is always zero in collisions, there exist for this model equilibrium states verifying (3.6), so that average quantities such as the N_α's, for instance, may depend on the space coordinates. However, we have restricted our investigation to the homogeneous equilibrium states. This implies that

$$\sum_{E\in\{E\}} P_0(E) \sum_i (a_{ij} - c_{ij}) \tag{3.6}$$

does not depend on j and

$$\sum_{E\in\{E\}} P_0(E) \sum_j (b_{ij} - d_{ij}) \tag{3.7}$$

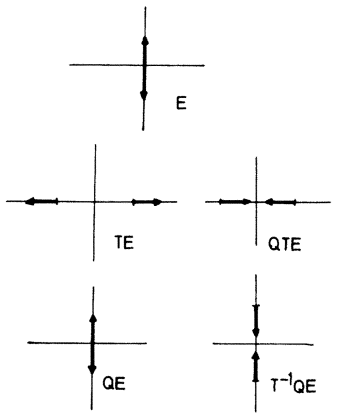

FIG. 3. Example of two colliding particles in an empty lattice.

does not depend on i.

Since P_0 is time invariant [which means that $P_0(TE) = P_0(E)$, for each E], the properties (3.6) and (3.7) will be conserved during the evolution. When these conditions are fulfilled, the equilibrium measure P_0 is

$$P_0(E) = \prod_{(i,j)\in\Lambda} \rho_1(a_{ij})\rho_2(b_{ij})\rho_3(c_{ij})\rho_4(d_{ij}), \tag{3.8}$$

where Λ represents the finite domain of observation and

$$\rho_\alpha(\lambda) \equiv \lambda N^0_\alpha + (1-\lambda)(1-N^0_\alpha), \tag{3.9}$$

the N^0_α being defined by (3.2), where P is replaced by P_0.

Let us remark that there is no correlation between different sites. Inserting (3.8) and (3.9) into (3.6), the four quantities N^0_α can be expressed in terms of n^0, J^0_x, and J^0_y,

$$N^0_1 = \tfrac{1}{4}n^0 + \tfrac{1}{2}J_x + \chi^0, \tag{3.10a}$$

$$N^0_2 = \tfrac{1}{4}n^0 + \tfrac{1}{2}J^0_y - \chi^0, \tag{3.10b}$$

$$N^0_3 = \tfrac{1}{4}n^0 - \tfrac{1}{2}J_x + \chi^0, \tag{3.10c}$$

$$N^0_4 = \tfrac{1}{4}n^0 - \tfrac{1}{2}J_y - \chi^0, \tag{3.10d}$$

the quantity χ^0 being itself a complicated function of n^0, J^0_x, and J^0_y. In the computer experiment, we have taken the macroscopic current to be zero; in this case,

$$\chi^0 = 0 \tag{3.11}$$

and

$$N^0_1 = N^0_2 = N^0_4 = N^0_3 = \tfrac{1}{4}n^0. \tag{3.12}$$

After having defined the equilibrium we shall investigate the dynamical behavior of the model. We introduce first the idea of a time-dependent hydrodynamical field. It is defined from a time-dependent "one-body distribution function"

$$N_1(i,j;t) = \sum_{E\in\{E\}} P(E)a_{ij}(T^tE), \tag{3.13a}$$

$$N_2(i,j;t) = \sum_{E\in\{E\}} P(E)b_{ij}(T^tE), \tag{3.13b}$$

$$N_3(i,j;t) = \sum_{E\in\{E\}} P(E)c_{ij}(T^tE), \tag{3.13c}$$

$$N_4(i,j;t) = \sum_{E\in\{E\}} P(E)d_{ij}(T^tE), \tag{3.13d}$$

and

$$n(i,j;t) = \sum_{\alpha=1}^{4} N_\alpha(i,j;t), \tag{3.14a}$$

$$J_x(i,j;t) = N_1(i,j;t) - N_3(i,j;t), \tag{3.14b}$$

$$J_y(i,j;t) = N_2(i,j;t) - N_4(i,j;t). \tag{3.14c}$$

The dynamics lead to local conservation relations,

$$n(i,j;t+1) = N_1(i-1,j;t) + N_2(i,j-1;t) + N_3(i+1,j;t) + N_4(i,j+1;t), \tag{3.15a}$$

$$J_x(i,j;t+1) = N_1(i-1,j;t) - N_3(i+1,j;t), \tag{3.15b}$$

$$J_y(i,j;t+1) = N_2(i,j-1;t) - N_4(i,j+1;t). \tag{3.15c}$$

Equations (3.15) give the laws of evolution for the hydrodynamic field. But under this form, they are just formal relations, as the exact nonequilibrium measure P is unknown; we shall give only an approximation of P in the case of weak gradients in space and time of the density and momentum density. In this hydrodynamical limit, we may approximate P by a pseudoinvariant measure P'_0

$$P'_0(E) = \prod_{(i,j)\in\Lambda} \rho'_1(a_{ij}(E))\rho'_2(b_{ij}(E)) \times\rho'_3(c_{ij}(E))\rho'_4(d_{ij}(E)), \tag{3.16}$$

where

$$\rho'_\alpha(\lambda) = 1 - \lambda + (2\lambda - 1)N^0_\alpha(i,j;t), \tag{3.17}$$

and where the quantities denoted by $N^0_\alpha(i,j;t)$ are defined as in (3.10), but here the number density and the momentum density depend on time and position.

The measure P'_0 is the so-called local equilibrium measure. Replacing P by P'_0 in (3.15), one finds the Euler fluid conservation equations, which take a rather unusual form in our model, the derivatives being replaced by finite differences,

$$\frac{\Delta n}{\Delta t} = -\left(\frac{\Delta J_x}{\Delta x} + \frac{\Delta J_y}{\Delta y}\right), \tag{3.18a}$$

$$\frac{\Delta J_x}{\Delta t} = -\frac{1}{2}\frac{\Delta n}{\Delta x}, \tag{3.18b}$$

$$\frac{\Delta J_y}{\Delta t} = -\frac{1}{2}\frac{\Delta n}{\Delta y}. \tag{3.18c}$$

In these equations, the second derivatives of the hydrodynamical field are neglected. As usual, the transport coefficients appear to next order in the development with respect to the gradients, namely, at the Navier-Stokes order. A number of methods exist for deriving these equations: the Green-Kubo[4] method, which is more systematic, but owing to the complicated dependence of χ^0 with respect to the hydrodynamical field we prefer to use the Landau-Lifschitz[5] fluctuating

hydrodynamics. According to this theory, one assumes that the long-wavelength fluctuations obey the usual linearized hydrodynamic equations, where a random strain is added in order to maintain at a constant level the static fluctuation; similarly, in the well-known Langevin theory a random force is added to the equation of motion of a small Brownian sphere in a viscous fluid, in order to assure that the velocity fluctuations of the sphere have at any time the Maxwell-Boltzmann distribution at the constant fluid temperature. The relation which then exists between the correlation of the random strain and the damping coefficient of the macroscopic equation yields the Green-Kubo formula. Near the state without average velocity, the only possible phenomenological equations are, owing to the symmetries of the system,

$$\frac{\Delta n}{\Delta t} = -\left(\frac{\Delta J_x}{\Delta x} + \frac{\Delta J_y}{\Delta y}\right), \tag{3.19a}$$

$$\frac{\Delta J_x}{\Delta t} = -\frac{1}{2}\frac{\Delta}{\Delta x}\left[n + \Theta\left(\frac{\Delta J_x}{\Delta x} - \frac{\Delta J_y}{\Delta y}\right)\right], \tag{3.19b}$$

$$\frac{\Delta J_y}{\Delta t} = -\frac{1}{2}\frac{\Delta}{\Delta y}\left[n + \Theta\left(\frac{\Delta J_y}{\Delta y} - \frac{\Delta J_x}{\Delta x}\right)\right]. \tag{3.19c}$$

The transport coefficient Θ accounts for the irreversible behavior of the many-body system, and it must be positive (if it exists) from elementary stability considerations. If Θ exists (and it turns out that it does not), Eq. (3.19) are valid in the Enskog expansion up to the second order in the gradients of the hydrodynamical field.

As explained above, the long-wavelength fluctuations of the hydrodynamical field obey the linearized equation (3.19), with an added random stress,

$$\frac{\Delta n}{\Delta t} = -\left(\frac{\Delta J_x}{\Delta x} + \frac{\Delta J_y}{\Delta y}\right), \tag{3.20a}$$

$$\frac{\Delta J_x}{\Delta t} = -\frac{1}{2}\frac{\Delta}{\Delta x}\left[n + \Theta\left(\frac{\Delta J_x}{\Delta x} - \frac{\Delta J_y}{\Delta y}\right) + F\right], \tag{3.20b}$$

$$\frac{\Delta J_y}{\Delta t} = -\frac{1}{2}\frac{\Delta}{\Delta y}\left[n + \Theta\left(\frac{\Delta J_y}{\Delta y} - \frac{\Delta J_x}{\Delta x}\right) - F\right]. \tag{3.20c}$$

These phenomenological equations are solved at once by use of the Fourier transform of the space-dependent fluctuations, defined as

$$\tilde{G}(\vec{k}; t) = \sum_{\vec{r}=(i,j)\in\Lambda} e^{-2i\vec{k}\cdot\vec{r}}\,[G(\vec{r}; t) - \langle G(\vec{r}; t)\rangle_0], \tag{3.21}$$

where Λ is the domain defined in (3.8) and $\langle G(\vec{r}; t)\rangle_0$ is the equilibrium value of $G(\vec{r}; t)$. In the long-wavelength limit

$$\vec{k} = (k_x, k_y) = k(\cos\varphi, \sin\varphi), \quad k \to 0,$$

we get

$$\Delta\tilde{n}/\Delta t = -2ik(\cos\varphi\tilde{J}_x + \sin\varphi\tilde{J}_y), \tag{3.22a}$$

$$\Delta\tilde{J}_x/\Delta t = -ik\cos\varphi\tilde{n} - 2k^2\cos^2\varphi\Theta\tilde{J}_x + 2k^2\sin\varphi\cos\varphi\Theta\tilde{J}_y + 2ik\tilde{F}\cos\varphi, \tag{3.22b}$$

$$\Delta\tilde{J}_y/\Delta t = -ik\sin\varphi\tilde{n} + 2k^2\sin\varphi\cos\varphi\Theta\tilde{J}_x - 2k^2\sin^2\varphi\Theta\tilde{J}_y - 2ik\tilde{F}\sin\varphi. \tag{3.22c}$$

This linear set of equations looks like a Langevin equation connecting the three fluctuating variables $(\tilde{n}, \tilde{J}_x, \tilde{J}_y)$; it is equivalent to three Langevin equations describing separarely the evolution of the normal modes. The first two modes are the sound waves with the amplitude $\tilde{u}_s$,

$$\tilde{u}_s = \epsilon\tilde{n}/\sqrt{2} + \tilde{J}_x\cos\varphi + \tilde{J}_y\sin\varphi + O(k), \tag{3.23}$$

with $\epsilon = \pm 1$. The Langevin equation for the fluctuating sound waves is

$$\Delta\tilde{u}_s/\Delta t = [-ik\epsilon\sqrt{2} - k^2\cos^2 2\varphi\Theta + O(k^2)]\tilde{u}_s + 2ik\tilde{F}\cos 2\varphi. \tag{3.24}$$

The amplitude of the mode of vorticity diffusion is

$$\tilde{u}_v = -\tilde{J}_x\sin\varphi + \tilde{J}_y\cos\varphi, \tag{3.25}$$

and the corresponding Langevin equation is

$$\Delta\tilde{u}_v/\Delta t = [-8k^2\sin^2 2\varphi\Theta + O(k^2)]\tilde{u}_v - 2ik\tilde{F}\sin 2\varphi. \tag{3.26}$$

As explained above, in any Langevin-type theory the friction coefficient Θ and the autocorrelation function of the fluctuating force $\tilde{F}(t)$ are related to each other.

In the long-wavelength limit $\tilde{u}_v$ varies slowly with time and

$$\Delta\tilde{u}_v/\Delta t \equiv \tfrac{1}{2}[\tilde{u}_v(t+1) - \tilde{u}_v(t-1)]$$

may be replaced by $\tilde{u}_v(t+1) - \tilde{u}_v(t)$ for simplification, the difference between the two expressions being of order k^4 at least. Solving then (3.26), one finds

$$\tilde{u}_v(t) = (1 - 8k^2\sin^2 2\varphi\Theta)^t\,\tilde{u}_v(0) - 2ik\sin 2\varphi\sum_{t'=0}^{t-1}(1 - 8k^2\sin^2 2\varphi\Theta)^{t-t'-1}\tilde{F}(t'). \tag{3.27}$$

At equilibrium, the static fluctuations are time independent, so that

$$\langle \tilde{u}_v^2(t)\rangle_0 = \langle \tilde{u}_v^2(0)\rangle_0. \tag{3.28}$$

Furthermore, as usual in any Langevin-type theory, one assumes

$$\langle \tilde{F}(t)\tilde{u}_v(t')\rangle_0 = 0, \quad \text{for all } t \geq t'. \tag{3.29}$$

From (3.27)–(3.29) we get the mean quadratic fluctuation

$$\langle u_v^2(0)\rangle_0 = \frac{1}{4\Theta}\sum_{t=0}^{\infty}\langle \tilde{F}(t'=0)\tilde{F}(t)\rangle_0. \tag{3.30}$$

Evaluating then the fluctuation on the left-hand side of (3.30), from (3.25),

$$\langle u_v^2(0)\rangle_0 = \lim_{k\to 0}\langle(-J_x\sin\varphi + J_y\cos\varphi)^2\rangle_0 = nL^2. \tag{3.31}$$

By comparison of (3.31) with (3.30),

$$\Theta = \frac{1}{4nL^2}\sum_{t'=0}^{\infty}\langle F(t'=0)F(t')\rangle_0 \tag{3.32}$$

$$= \lim_{k\to 0}\left(\frac{1}{4nL^2}\sum_{t'=0}^{\infty}\left\langle\sum_{\vec{r}} e^{-2i\vec{k}\cdot\vec{r}}F(t'=0)\times\sum_{\vec{r}} e^{-2i\vec{k}\cdot\vec{r}}F(t)\right\rangle_0\right) \tag{3.33}$$

$$= \frac{1}{4nL^2}\sum_{t=0}^{\infty}\langle F(0)F(t)\rangle_0. \tag{3.34}$$

The fluctuating pressure can be expressed in a microscopic form; from (3.20) $F(t)$ changes its sign when the axes (x, y) are rotated $\frac{1}{2}\pi$; the only possible expression having this property is

$$F(t) = \frac{1}{\sqrt{N^2}}\sum_{i,j\in\Lambda}(a_{ij} - b_{ij} + c_{ij} - d_{ij})(T^tE). \tag{3.35}$$

Replacing (3.35) in (3.34) the Green-Kubo expression for the transport coefficient Θ, we get

$$\Theta = \frac{n}{L^2}\sum_{t=0}^{\infty}\left\langle\sum_{i,j\in\Lambda}(a_{ij} - b_{ij} + c_{ij} - d_{ij})(E)\times\sum_{i,j\in\Lambda}(a_{ij} - b_{ij} + c_{ij} - d_{ij})(T^tE)\right\rangle_0 \tag{3.36}$$

IV. RESULTS

The main object of this paper is to evaluate the time correlation function

$$\Psi(t) = \sum_{E\in\{E\}} P_0(E)F(E)F(T^tE), \tag{4.1}$$

which should be related to the transport coefficient by

$$\Theta = n\sum_{t=0}^{\infty}\Psi(t). \tag{4.2}$$

Actually, according to the arguments presented by de Pazzis,[6] the series $\sum_{t=0}^{\infty}\Psi(t)$ do not converge, except perhaps for $n=2$ (i.e., when two particles lie on the average at each vertex).

We also measured the time correlation functions

$$\nu_1(t) = \sum_{E\in\{E\}} P_0(E)[a_{ij}(T^tE) - n][a_{ij}(E) - n] \tag{4.3}$$

and

$$\nu_3(t) = \sum_{E\in\{E\}} P_0(E)[a_{ij}(T^tE) - n][a_{ij}(E) - n], \tag{4.4}$$

because there are theoretical predictions about their asymptotic behavior.[1] The computational method is explained in Appendix A.

The computations have been done on the Univac 1108 computer at the Orsay University; we measured $\Psi(r)$ and the velocity time correlations defined in (4.3)–(4.4), the number density being equal to $\frac{2}{3}$, 1, and 2 and the macroscopic velocity being set to zero.

A run for a given density required ~10 h. The results given in Figs. 4–11 in logarithmic scales show explicitly that the time correlations take the form Rt^{-s} at long times.

Each of these functions have been fitted by minimizing

$$\sum_{t=10}^{1000}(f(t) - Rt^{-s})^2. \tag{4.5}$$

In fact, we observed that the Rt^{-s} behavior begins

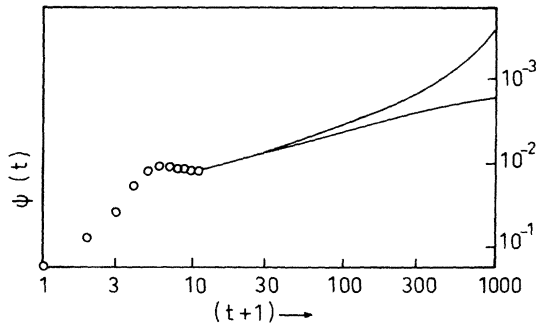

FIG. 4. $\psi(t)$ as a function of t on a log-log scale for $n = \frac{2}{3}$. For the lowest values of time, the experimental points are represented by circles, but when time increases these are so concentrated that we draw only the boundary of the area containing them.

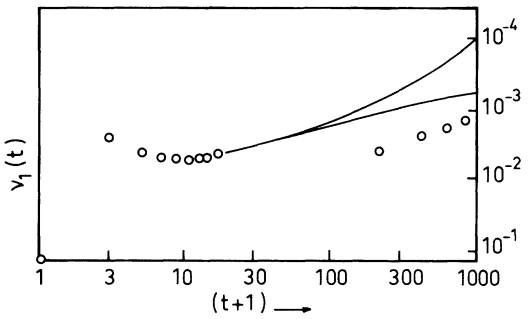

FIG. 5. ν_1 as a function of t on a log-log scale for $n=\frac{2}{3}$. Note the anomalous amplitude at $t=2K(L-1)$.

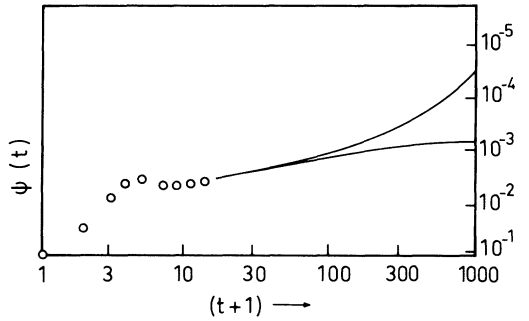

FIG. 7. $\psi(t)$ as a function of t on a log-log scale for $n=1$.

at $t=10$ at least (a mean free flight time). As we derived from a single set of data the two quantities R and S, the errors on R and S are not independent.

To give an idea of the accuracy we have plotted in Figs. 12–19 in the plane R, S the curve for which (4.5) equals twice its minimum value. The area inside this curve may be taken as the domain of adequate values of R and S. The best values of the two parameters are given in Tables I–III.

We have not yet obtained any definite result concerning the behavior of $\Psi(t)$ at the density $n=2$; in fact, this function of time decreases very rapidly and its amplitude becomes of the order of the noise at times of order of or larger than a few units. Actually the theoretical analysis which was performed by de Pazzis[6] proved that $\Psi(t)$ is exactly zero at times 1 and 2 and that $\Psi(t)$ decreases at this density as $t^{-3/2}$ at long times.

This situation is quite unfortunate, since Θ should exist in this case. We believe that the best way to study $\Psi(t)$ at density 2 is to compute its value exactly, if possible. The calculation should be probably quite similar to (but more complicated than) the high-temperature expansion of the free energy of an Ising system on a square lattice.

Let us remark that for the results of densities $\frac{2}{3}$ and 1 the value of the exponents S are larger than $\frac{1}{2}$. This may be explained as follows: Assuming that Θ exists, a Landau-Placzek-type calculation given an asymptotic law[6] as $(\Theta t)^{-1/2}$ for $\Psi(t)$, but this is self-contradictory and shows that Θ is infinite. It is then more natural to expect that the actual value of S is larger than $\frac{1}{2}$.

It should be noted that one can derive from the microscopic equations the exact values of $\Psi(t)$, $\nu_1(t)$, and $\nu_3(t)$ for $t=0, 1, 2$. As an example, let us calculate $\nu_1(0)$. From (4.3),

$$\nu_1(0)=\langle(a-n)^2\rangle_0=\langle a^2-2an+n^2\rangle_0. \tag{4.6}$$

From $\langle a\rangle=\frac{1}{4}n$ and $a^2=a$ ($a=0$ or 1),

$$\nu_1(0)=\tfrac{1}{4}n(1-\tfrac{1}{4}n). \tag{4.7}$$

The exact values of $\Psi(t)$, $\nu_{1,3}(t)$ at $t=0, 1, 2$ are listed on Table IV and are compared in Tables V–VII with the experimental ones.

In Figs. 5, 8, and 10, giving $\nu_1(t)$ at different densities, one can observe at times $t=2(L-1)$, $t=4(L-1)$, $t=6(L-1)$, and $t=8(L-1)$ an anomalously large amplitude of the time correlation function $\nu_1(t)$. This can be explained by the form of the periodic boundary conditions. In fact, in

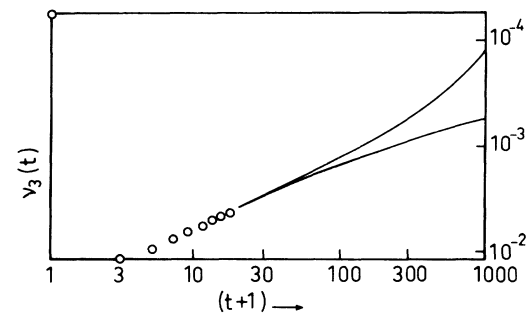

FIG. 6. ν_3 as a function of t on a log-log scale for $n=\frac{2}{3}$.

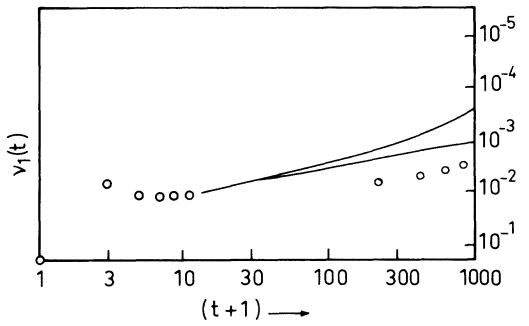

FIG. 8. ν_1 as a function of t on a log-log scale for $n=1$. Note the anomalous amplitude at $t=2K(L-1)$.

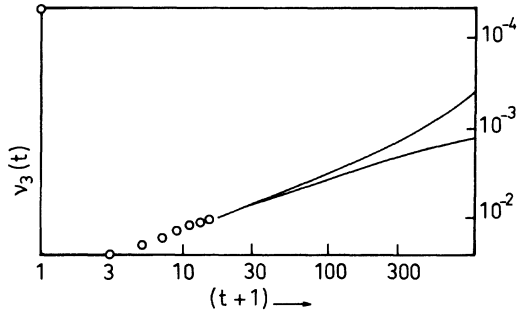

FIG. 9. ν_3 as a function of t on a log-log scale for $n=1$.

the torus Λ the points $[i+h(L-1), j+h'(L-1)]$ are identical (for h and h' integers) to $[i,j]$, and the velocity correlations obtained from a system on the torus are the same as the ones which could be obtained in a larger domain $\Lambda' \gg \Lambda$, except that it contains the contribution of the image points in the torus Λ,

$$\nu_1^*(h,h';t)=\sum_{E\in\{E\}} P_0(E)[a_{ij}(T^tE)-n][a_{lm}(E)-n], \tag{4.8}$$

where

$$i=l+h(L-1), \quad j=m+h'(L-1).$$

Generally, the contribution of the image fluctuations is quite small, but as it has been proved,[6] $\nu_1^*(h,h';t)$ decreases very slowly in the domain $|i-l|+|j+m|=t$.

At $t=2(L-1)$ the velocity correlation function $\nu_1(t)$ takes a value very different from that in a greater domain Λ', but for $t<2(L-1)$ the difference disappears. The $\nu_1^*(h,h';t)$ being proved to behave like $t^{-1/2}$, on the logarithmic scales of Figs. 5, 8, and 10 the points representing $\nu_1(t)$ at $t=2(L-1)$, $4(L-1)$, $6(L-1)$, and $8(L-1)$ are expected to lie on a line, denoting a behavior like

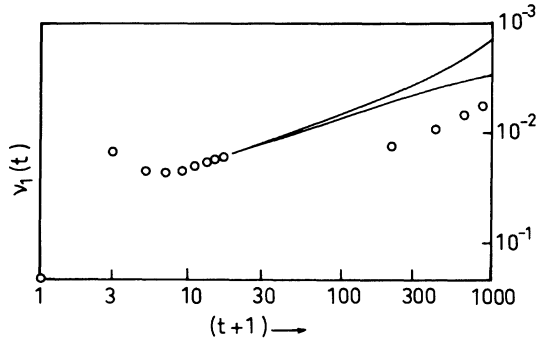

FIG. 10. ν_1 as a function of t on a log-log scale for $n=2$. Note the anomalous amplitude at $t=2K(L-1)$.

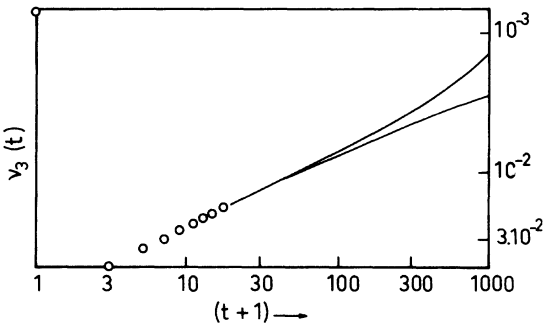

FIG. 11. ν_3 as a function of t on a log-log scale for $n=2$.

$t^{-1/2}$ (approximately); this point can be verified and the line is (approximately) parallel to the one where the values of $\nu_1(t)$ are represented at different times. In some sense, the anomalous behavior of $\nu_1(t)$ arises from the fact that there is no damping of the sound waves (in the Navier-Stokes approximation) if the direction of the wave vector $\vec{k}$ is parallel to one of the bisectors of the lattice.

The same anomalous behavior holds for $\nu_3(t)$, but as shown in Ref. 1,

$$\nu_3^*(h,h';t)=\sum_{E\in\{E\}} P_0(E)[a_{ij}(T^tE)-n][c_{lm}(E)-n], \tag{4.9}$$

where

$$i=l+h(L-1), \quad j=m+h'(L-1),$$

decreases as $t^{-3/2}$ when $2h(L-1)=t$ and $\nu_3(t)$ decreases as $t^{-1/2}$ (approximately); the steps at $t=2(L-1)$ are not appreciable.

From Ref. 1, the values of $\nu_1^*(1,1;t)$ can be written

$$\nu_1^*(1,1;t)=\frac{2\sqrt{2\pi}}{\pi^2}\,\frac{\mu^2}{[\mu(1-\mu)]^{1/2}}\,\frac{1}{\sqrt{t}}. \tag{4.10}$$

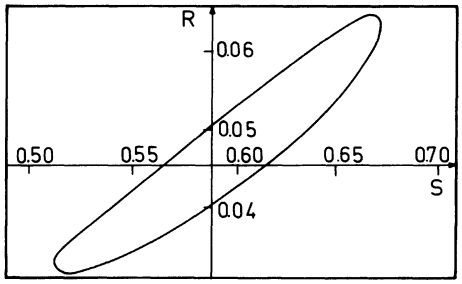

FIG. 12. Accuracy domain of R and S for $\psi(t)$, the density being equal to $\frac{2}{3}$.

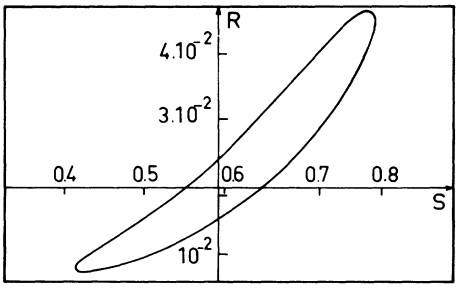

FIG. 13. Accuracy domain of R and S for $\nu_1(t)$, the density being equal to $\frac{2}{3}$.

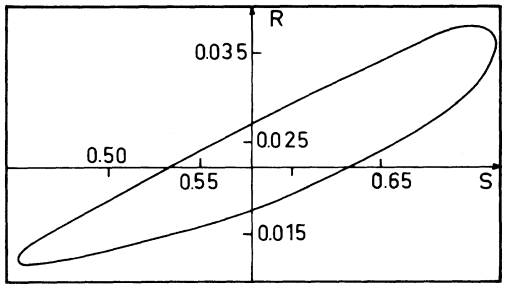

FIG. 15. Accuracy domain of R and S for $\psi(t)$, the density being equal to 1.

The values ν_1(experimental) $+ \nu_1^*(1, 1; t)$ (theoretical) are compared with $(\nu_1 + \nu_1^*)$ (experimental) in Table VIII.

As a conclusion, let us stress that this model allows one to check with good accuracy various theoretical predictions about the asymptotic behavior of time correlations in a classical two-dimensional fluid. In our opinion this model could also serve to generate random numbers; for instance, the fluctuations of a random variable such as the quantity denoted by $F(E)$ have been shown to be almost completely uncorrelated at different times. We intend to explore this point in the future.

APPENDIX A

This appendix is concerned with computation, and the discrete nature led us to develop rather unusual methods. The notation used in (2.2) suggests the construction of four vectors A_m, B_m, C_m, and D_m whose components are equal to zero or one and are obtained by setting the microscopic velocities $(a_{ij}, b_{ij}, c_{ij}, d_{ij})$ in alphabetical order.

Since the observation domain Λ chosen is a square on the lattice with its sides of length L approximately parallel to the directions of the lattice, the components of the vectors A_m, B_m, C_m, and D_m are related to a configuration of the system by

$$A_m = A_{i+jL} \equiv a_{ij}, \quad B_m = B_{i+jL} \equiv b_{ij}, \qquad C_m = C_{i+jL} \equiv c_{ij}, \quad D_m = D_{i+jL} \equiv d_{ij}, \tag{A1}$$

with $1 \leq i, j \leq L$ and $1 \leq s = i + jL \leq L^2$. Any vector of the set $\{A_m, B_m, C_m, D_m\}$ records the position of particles moving in a given direction.

Instead of recording positions and velocities of each particle separately, we recorded the whole space of configuration E, particles as well as holes. Since in FORTRAN the words are made of 36 bits, we recorded the A_m, for example, by $\frac{1}{36}L^2$ words, any binary digit denoting a particle or a hole according to whether it is equal to 1 or zero, respectively. For a reason given below the observation domain Λ has been chosen to be the largest one which is compatible with the capacity of the computer memory cells. The length of the square sides is 108, so that the number of vertices is $(108)^2 = 11\,664$; at the density $n = 2$, 23 328 particles are in the system.

Before we describe the process of time evolution, let us explain how the initial condition is constructed. We have chosen the case where the average velocity is zero [if there are macroscopic currents, the Navier-Stokes equations and the Green-Kubo formula are no longer valid in the

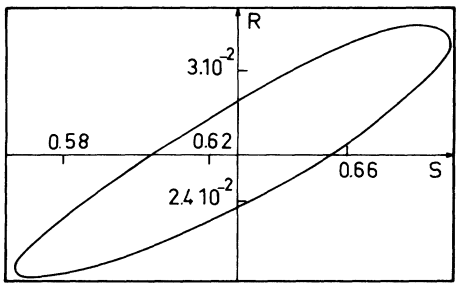

FIG. 14. Accuracy domain of R and S for $\nu_3(t)$, the density being equal to $\frac{2}{3}$.

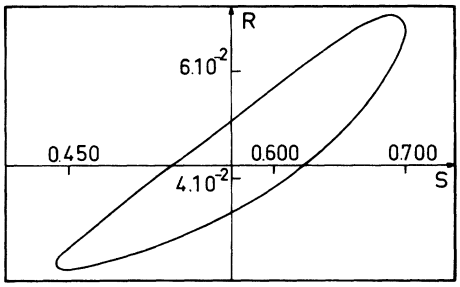

FIG. 16. Accuracy domain of R and S for $\nu_1(t)$, the density being equal to 1.

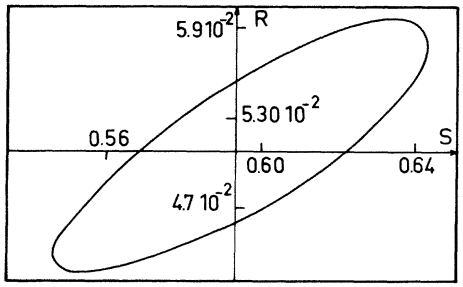

FIG. 17. Accuracy domain of R and S for $\nu_3(t)$, the density being equal to 1.

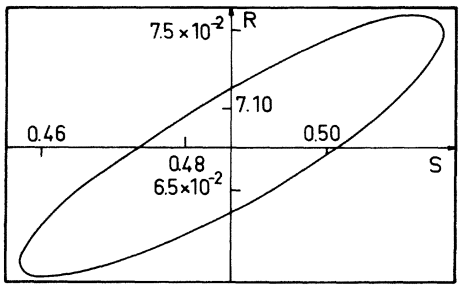

FIG. 19. Accuracy domain of R and S for $\nu_3(t)$, the density being equal to 2.

form given in (3.19) and (3.36); they must be replaced by other, more complicated expressions].

To simplify the construction of the initial condition we took

$$\sum_{m=1}^{L^2} A_m = \sum_{m=1}^{L^2} B_m = \sum_{m=1}^{L^2} C_m = \sum_{m=1}^{L^2} D_m = \frac{nL^2}{4}, \quad \text{(A2)}$$

so that the initial fluctuation $F(E)$ is just zero. The initial configuration is constructed as follows: One takes a strictly positive random integer (r) smaller than L^2; if there is no particle at point (r) (the bit A_r equals zero) a particle is put there (the bit is changed to 1); if there is a particle (the bit equals 1) another point is chosen at random and the process is continued for as long as $\sum_{m=1}^{L^2} A_m = \frac{1}{4} nL^2$; the initial vectors B, C, and D are constructed similarly. From this initial configuration E, one can get successively $TE, T^2E, \ldots, T^nE$ by applying the evolution laws. In doing this, it is important to remember that the evolution operator T is the product of a collision operator C and of a free translation operator T_0; thus we shall describe separately the two processes.

There are only two dynamical situations at a vertex for which a collision occurs,

$$\{A_m B_m C_m D_m\} = 1010 \text{ or } 0101. \quad \text{(A3)}$$

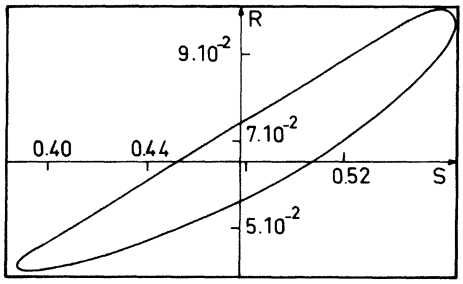

FIG. 18. Accuracy domain of R and S for $\nu_1(t)$, the density being equal to 2.

In order to define the result of a collision we have introduced $\mathfrak{A}$ and Θ as

$$\mathfrak{A}(A_m, B_m) = A_m B_m, \text{ for every } A_m, B_m \in \{0, 1\}, \quad \text{(A4)}$$

and

$$\Theta(A_m, B_m) = \begin{cases} 1, & \text{if } A_m B_m = 10 \text{ or } 01, \\ 0, & \text{otherwise.} \end{cases} \quad \text{(A5)}$$

Thus one can express the collision law by

$$\hat{C}(A_m, B_m, C_m, D_m) = (\Theta(A_m, U_m), \Theta(B_m, U_m), \Theta(C_m, U_m), \Theta(D_m U_m)), \quad \text{(A6)}$$

for every $m \in \{1, 2, 3, \ldots, L^2\}$, with

$$U_m = \mathfrak{A}[\mathfrak{A}\{\Theta(A_m, B_m), \Theta(C_m, D_m)\}, \Theta\{A_m, (1 - C_m)\}].$$

Since the logical operations are performed simultaneously between bits of same ranks in the FORTRAN words made up of 36 bits, the nine logical operations required in (A6) allow us to perform collision on 36 sites in parallel; for the whole system the construction of $\hat{C}E$ from E then requires $9(\frac{1}{36} L^2)$ (=2926 if $L = 108$) logical operations.

Before defining the translation law we have to set boundary conditions, leaving invariant the dynamically conserved quantities (i.e., the num-

TABLE I. Best values of R, S, where $\Psi(t), \nu_1(t), \nu_3(t) = Rt^{-S}$ [cf. Eq. (4.5)], for $n = \frac{2}{3}$.

	$\Psi(t)$	$\nu_1(t)$	$\nu_3(t)$
R	0.0452	0.02	0.0262
S	−0.589	−0.583	−0.628
Accuracy for S	3%	8%	3%

TABLE II. Same as for Table I, but with $n=1$.

	$\Psi(t)$	$\nu_1(t)$	$\nu_3(t)$
R	0.0224	0.0425	0.0507
S	−0.578	−0.568	−0.593
Accuracy for S	9%	8%	4%

ber of particles and the mean velocity). We have chosen helicoidal boundary conditions, so that the laws (2.4) are translated by

$$T_0 A_m = A_{\{(m-2+L^2) \bmod L^2+1\}},$$

$$T_0 B_m = B_{\{(m-L-1+L^2) \bmod L^2+1\}},$$

$$T_0 C_m = C_{\{m \bmod L^2+1\}}, \quad T_0 D_m = D_{\{(m+L-1) \bmod L^2+1\}},$$

for every $m \in \{1, 2, 3 \ldots L^2\}$. To give an idea of the meaning of these boundary conditions, one may imagine that the system is made of four ordered sets of L^2 bits, namely, $\{A_m, B_m, C_m, D_m\}$, which are arranged on four circles. During the free translation the circle A turns one computer bit clockwise, the circle B turns L bits clockwise, the circle C turns one bit counterclockwise, and the circle D turns L bits counterclockwise. The boundary conditions defined implicitly by (4.9) are a little different from the usual periodic boundary conditions, which should be, for every $(i,j) \in \Lambda$,

$$T_0 a_{ij} = a_{\{(i-2+L) \bmod L+1\}j}, \quad T_0 b_{ij} = b_{i\{(j-2+L) \bmod L+1\}},$$
$$T_0 C_{ij} = C_{\{i \bmod L+1\}j}, \quad T_0 d_{ij} = d_{i\{j \bmod L+1\}}. \tag{A8}$$

With our helicoidal boundary conditions, the directions of the sides of the torus of observation Λ and the direction of the lattice are not exactly parallel, the angle between them being $\tan^{-1}(1/L)$ (see Fig. 20).

A particle escaping the domain Λ toward the right-hand side will be reintroduced on the left-hand side a line below, although under the boundary conditions (A8) it should be reintroduced at the same line. However, we have done a few computations with the boundary conditions (A8);

TABLE III. Same as for Table I, but with $n=2$.

	$\nu_1(t)$	$\nu_3(t)$
R	0.0650	0.0668
S	−0.478	−0.486
Accuracy for S	6%	3%

TABLE IV. Exact values for Ψ, $\nu_{1,3}$ at $t=0,1,2$. $\mu = \frac{1}{4}n(1-\frac{1}{4}n)$.

t	Ψ	ν_1	ν_3
0	μ	μ	0
1	$\mu(1-4\mu)$	0	0
2	$\mu(1-4\mu)^2$	μ^3	$\mu^2(1-\mu)$

there is no marked difference in the final results except that the boundary conditions (A8) are more time consuming than (A7).

Practically, $\Psi(t)$, $\nu_1(t)$, and $\nu_3(t)$ are not computed from their initial definitions (4.1), (4.3), and (4.4); one replaces the ensemble average by an average over a single trajectory of the system at different times,

$$\Psi(t) = \lim_{M\to\infty} \frac{1}{M} \sum_{t'=1}^{M} F(T^{t'}E)F(T^{t+t'}E), \tag{A9}$$

$$\nu_1(t) = \lim_{M\to\infty} \frac{1}{M} \sum_{t'=1}^{M} [a_{ij}(T^{t+t'}E)-n][a_{ij}(T^{t'}E)-n], \tag{A10}$$

$$\nu_3(t) = \lim_{M\to\infty} \frac{1}{M} \sum_{t'=1}^{M} [a_{ij}(T^{t+t'}E)-n][a_{ij}(T^{t'}E)-n]. \tag{A11}$$

The definitions (A9)–(A11) are equivalent to (4.1), (4.3), and (4.4), provided that the system has good ergodic properties, as we shall show.

The method for calculating the velocity time correlations $\nu_1(t)$ and $\nu_3(t)$ follows at once from (A10) and (A11); however, there are some tricks which save computational time in calculating $\Psi(t)$. As $F(t)$ changes only when collisions occur, we have

TABLE V. Comparison of theoretical and experimental values of Ψ. $\nu_{1,3}$, for $t=0,1,2$, with density of $\frac{2}{3}$.

	Theory	Expt.
$\Psi(0)$	0.14	0.14
$\Psi(1)$	6.2×10^{-2}	6.7×10^{-2}
$\Psi(2)$	2.7×10^{-2}	3.2×10^{-2}
$\nu_1(0)$	1.4×10^{-1}	1.2×10^{-1}
$\nu_1(1)$	0	0
$\nu_1(2)$	2.67×10^{-3}	2.03×10^{-3}
$\nu_3(0)$	0	5.0×10^{-5}
$\nu_3(1)$	0	0
$\nu_3(2)$	1.66×10^{-2}	1.17×10^{-2}

TABLE VI. Same as for Table V, but for density of 1.

	Theory	Expt.
$\Psi(0)$	0.19	0.19
$\Psi(1)$	4.7×10^{-2}	4.3×10^{-2}
$\Psi(2)$	1.2×10^{-2}	1.0×10^{-2}
$\nu_1(0)$	0.19	0.18
$\nu_1(1)$	0	0
$\nu_1(2)$	6.59×10^{-3}	6.2×10^{-3}
$\nu_3(0)$	0	3.9×10^{-5}
$\nu_3(1)$	0	0
$\nu_3(2)$	2.8×10^{-2}	2.5×10^{-2}

$$F(T^t E) - F(E) = 2n \sum_{m=1}^{L^2} \{ \mathcal{C}[A_m(E), U_m(E)] - \mathcal{C}[B_m(E), U_m(E)] \}. \tag{A12}$$

Since the collision frequency is less than 1, it is actually faster to compute $\Psi(t)$ from (A12) than to perform at each step, the lattice summation implied in the definition of $F(E)$ in (3.36).

APPENDIX B

This appendix deals with the problems of computational errors. Although the nature of the model itself eliminates any error in the dynamics and in the computation of any dynamical quantity, a source of difference between our results and the exact ones remains, as we cannot make averages over an infinite system. An approximation

TABLE VIII. Anomalous amplitude of $\nu_1(t)$: comparison between theory and experiment [cf. Eq. (4.10)], for $n = 2, 1$, and $\frac{2}{3}$.

	n		
	2	1	$\frac{2}{3}$
Theory	1.02×10^{-2}	4.79×10^{-3}	3.81×10^{-3}
Experiment	1.40×10^{-2}	6.40×10^{-3}	3.21×10^{-3}

of (A9) is

$$\Psi(M, t) = \frac{1}{M} \sum_{t'=1}^{M} F(T^{t'} E) F(T^{t+t'} E), \tag{B1}$$

where M must be as large as possible.

The function $\Psi(M, t)$ obtained has a well-defined part which corresponds to $\Psi(\infty, t) = \Psi(t)$ plus some random fluctuations. We shall see that the magnitude of these fluctuations depends on M and on the size of Λ. Since the correlation function $\Psi(t)$ vanishes when t increases, $\Psi^2(M, \infty)$ may measure the computational error on $\Psi(M, t)$. From (B1),

$$\Psi^2(M, t) = \frac{1}{M} \sum_{t'=1}^{M} \sum_{t''=1}^{M} F(T^{t'} E) F(T^{t''} E) \times F(T^{t+t'} E) F(T^{t+t''} E), \tag{B2}$$

and then when t goes to infinity,

$$\Psi^2(M, t) \xrightarrow[t \to \infty]{} \frac{1}{M} \sum_{t'=1}^{M} [F(T^{t'} E) F(T^{t+t'} E)]^2. \tag{B3}$$

Coming back to the initial definition of $F(E)$, one can show the influence of the size of Λ:

$$\Psi^2(M, t) \xrightarrow[t \to \infty]{} \frac{1}{M} \sum_{t'=1}^{M} \left(\frac{1}{L^2} \sum_{m=1}^{L^2} \{A_m - B_m + C_m - D_m\}(T^{t'} E) \{A_1 - B_1 + C_1 - D_1\}(T^{t+t'} E) \right)^2. \tag{B4}$$

Since $A_m^2 = 1$, $|A_m - B_m + C_m - D_m| \leq 2$; the quantity

$$\{A_m - B_m + C_m - D_m\}(T^{t'} E) \{A_1 - B_1 + C_1 - D_1\}(T^{t+t'} E)$$

TABLE VII. Same as for Table VI, but for density of 2.

	Theory	Expt.
$\nu_1(0)$	0.25	0.24
$\nu_1(1)$	0	0
$\nu_1(2)$	1.5×10^{-2}	1.52×10^{-2}
$\nu_3(0)$	0	6.2×10^{-4}
$\nu_3(1)$	0	0
$\nu_3(2)$	4.7×10^{-2}	4.66×10^{-2}

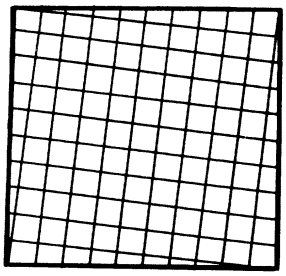

FIG. 20. Visualization of the periodic helicoidal boundary conditions.

may be considered as a random variable, since t tends to infinity and its mean quadratic fluctuation is smaller than 4. The law of large numbers shows that

$$\sum_{m=1}^{L^2} \{A_m - B_m + C_m - D_m\}(T^{t'}E) \times \{A_1 - B_1 + C_1 - D_1\}(T^{t+t'}E)$$

is a random variable with a variance proportional to L. From our numerical results $F(E)F(T^tE)$ behaves approximately as $t^{-1/2}$ for large times; thus

$$\Psi^2(M, \infty) \sim (1/L^2)(\ln M)/M . \tag{B5}$$

Since the computational time is proportional to M and L^2, it is more efficient to increase L than to increase M for minimizing fluctuations of $\Psi(M, t)$. This pecularity arises from the fact that the Green-Kubo integrand is not integrable.

[1]J. Hardy, O. De Pazzis, and Y. Pomeau, J. Math. Phys. 14, 1746 (1973).
[2]Y. Pomeau and P. Resibois, Phys. Rep. (to be published).
[3]J. L. Lebowitz, in Conference on Statistical Mechanics, Chicago University, March, 1971 (unpublished).
[4]J. Hardy and Y. Pomeau, J. Math. Phys. 13, 1042 (1972).
[5]L. D. Landau and I. Lifschitz, Zh. Eksp. Teor. Fiz. 32, 618 (1957) [Sov. Phys.—JETP 5, 512 (1957)]; also in *Collected Papers of Landau*, edited by D. ter Haar (Pergamon, New York, 1965).
[6]O. de Pazzis, Ph.D. thesis (University of Orsay, 1973) (unpublished).
[7]B. J. Alder and T. E. Wainwright, Phys. Rev. A 1, 18 (1970); Phys. Rev. Lett. 18, 988 (1967).